# Charged-particle emission accompanying muon capture by nuclei

Yu. A. Batusov and R. A. Éramzhyan

*Joint Institute for Nuclear Research, Dubna*
Fiz. Elem. Chastits At. Yadra. 8, 229–254 (March–April 1977)

The experimental data on the emission of charged particles when muons are captured by nuclei are systematized and considered from the theoretical point of view.

PACS numbers: 25.30.Ei

## INTRODUCTION

For a long time, one of the most pressing problems in nuclear physics concerned the mechanism of muon absorption by nuclei. The experimental confirmation of the idea that collective states of the nuclei play a dominant role in this process made it possible to understand and explain on a unified basis the main features of the process. Questions relating to the capture mechanism are no longer so pressing and have given place to new problems brought forward by the experiments: the description of the energy spectra of the products of disintegration (in the first place, neutrons) of nuclei resulting from the absorption of muons, their angular distributions, the probabilities of population of the various states of the daughter nuclei, and so forth. This shift of interests has not come about by chance. The description of nuclear disintegration processes has a profound bearing on many aspects of nuclear structure and reaction mechanisms and makes it possible to test from all sides many conceptions that form the basis of the theory of the interaction between muons and nuclei.

Among the various disintegration channels of a nucleus that captures muons, channels with the emission of charged particles play a particular role. The emission of such particles is not directly related to the elementary event of muon capture but is due to the existence in the nucleus of correlations between the nucleons. On the one hand, the correlations lead to the formation in the nucleus of various collective states. The muon capture takes place predominantly through collective states of the giant resonance type. In a number of cases, the decay of these states leads to the emission of charged particles. This immediately prompts one of the main questions: To what extent is the emission of charged particles in muon capture due to the decay of resonance states?

On the other hand, short-range correlations lead to clustering of the nucleons in the nucleus. The interaction of muons with such subsystems is more complicated and may lead, as experimental investigation of other processes shows, to the appearance of particular disintegration channels with the emission of several correlated particles.

The first information about charged particles emitted as a result of muon capture by nuclei was obtained long ago in cosmic-ray experiments.[1] The systematic study of this process began quite recently. The experimental and theoretical information that has now been accumulated[2] requires systematization and examination from the point of view of theoretical interpretation. This is the subject of the present paper.

## 1. EXPERIMENTAL YIELDS OF CHARGED PARTICLES RESULTING FROM MUON CAPTURE BY NUCLEI

Muon capture by nuclei with the emission of charged particles can be studied effectively by the method of nuclear photoemulsions. Its use has made it possible to determine the probability of events with the emission of charged particles and establish some general features of the process.[3–6] The results of measurements of the probability $w_\sigma$ of emission of charged particles when muons are captured by nuclei of the photoemulsion are given in Table I. Taken as a whole, they agree with one another, and in the two cases of Refs. 4 and 6 agree very well. The mean value of these two measurements is $w_\sigma = (1.95 \pm 0.06)\%$. The slightly larger value of $w_\sigma$ given in Refs. 3 and 5 may be due to the insufficiently accurate allowance for background events, which are due primarily to the admixture of pions in the muon beam. These admixtures are usually small. However, because approximately 70% of the endings of pions in the photoemulsion are accompanied by the emission of charged particles,[7] their resulting contribution may be large.

The distribution of $\sigma$ stars[1)] from the capture of muons by nuclei is shown in Table II. In it, $N_n/N$ is the ratio in percentages of the number of $n$-prong stars to the total number of $\sigma$ stars. Capture of a muon by the light component of the emulsion (C, N, and O) with the emission of one charged particle corresponds, as a rule, to a two-prong $\sigma$ star, in which one of the prongs is formed by the recoil nucleus. The emission of a further heavy neutral particle at definite emission angles may lead to a distribution of the momenta in which the recoil nucleus remains almost at rest. In this or a similar case, the capture of muons by the light component of the emulsion leads to the appearance of single-prong stars. However, the probability of these events is of course small. In a first approximation, therefore,

[1)] Stoppings of muons in the emission with their subsequent capture by nuclei accompanied by the emission of charged particles are called $\sigma$ stoppings, and the corresponding stars, $\sigma$ stars.

 0090-4759/77/0802-0095$02.80  

TABLE I. Yield of charged particles per capture event in the nuclear photoemulsion.

| Number of muon stoppings | Yield of charged particles, % | Reference |
|---|---|---|
| $2.4 \cdot 10^4$ | 2.4 | [3] |
| $9.3 \cdot 10^4$ | 1.95±0.07 | [4] |
| $\sim 1 \cdot 10^6$ | 1.94±0.11 | [6] |
| $(2.74 \pm 0.14) \cdot 10^5$ | 3 | [5] |

TABLE II. Pron distribution of σ stars, $N_n/N(\%)$, from muon capture by nuclei of the photoemulsion.

| Number of prongs $n$ | | | | | Reference |
|---|---|---|---|---|---|
| 1 | 2 | 3 | 4 | 5 | |
| 70.7±3.6 | 24.6±2.1 | 3.6±0.8 | 0.9±0.4 | 0.2±0.2 | [3] |
| 86.5 | 10.3 | 2.8 | 0.3 | 0.06 | [4] |
| 69.0±2.3 | 21.4±1.3 | 7.9±0.8 | 1.6±0.3 | 0.1±0.1 | [5] |
| 78.5±1.6 | 14.8±0.7 | 5.2±0.4 | 1.5±0.2 | 0.03±0.03 | [8] |

all the experimentally observed single-prong σ stars can be attributed to capture by the heavy component (Ag, Br) of the photoemulsion.[3,4]

The probability of the events associated with each component of the photoemulsion separately can be determined by using the standard criteria[9] of the Coulomb barrier (as was done in Ref. 5) or Auger electrons[2)] (see Ref. 6). The results of evaluation of the experimental data on the basis of these criteria are given in Tables III and IV. The total yield of charged particles from the capture of muons by nuclei of the heavy component of the photoemulsions is the same in all measurements and amounts to about 3%. It is different for the light component, for which the discrepancies are rather serious (Table V).

The emitted charged particles have a short range, in rare cases exceeding 2000–3000 μm of emulsion (Fig. 1). It is therefore difficult in practice to distribute the particles according to masses. It is somewhat easier to distinguish the charges of the particles, though this could be done only in one case.[3] According to the results of Ref. 3, capture by the heavy component of the emulsion leads predominantly to the emission of singly charged particles (2.2% per muon-absorption event). The remaining 0.5% is made up of α particles. It was not possible to identify the singly charged particles from their masses. The probability of emission of singly charged particles in the case of the light component was found to be 9.5%; that of the α particles, 3.4%.

The singly charged particles were separated according to masses in Ref. 5. The results of the corresponding analysis are given in Table VI. It is interesting to note that the yields of protons and dueterons were found to be practically equal in the case of capture by the light component.

The emulsion method has proved fairly effective for studying channels with the emission of charged particles in muon capture by nuclei belonging to the emulsion, and it has yielded varied information, both quantitative and qualitative, about these processes. However, the entire information refers, not to an individual nucleus, but to a group of nuclei. For the heavy component (Ag, Br) this is not very important since in this region the individual features of the nuclei are usually manifested very weakly. It is different in the case of light nuclei, in which the individual features of their excitation frequently determine the type of decay. Measurements with high accuracy of the emission angles of the charged particles and their energies with subsequent kinematic analysis has made it possible to distinguish a number of channels and determine their probabilities[10,11]:

$$\left.\begin{array}{l} {}^{12}\mathrm{C}(\mu^-, \nu){}^{8}\mathrm{Li} + \begin{cases} {}^{4}\mathrm{He}, & w < 2.6 \cdot 10^{-2}\%; \\ {}^{3}\mathrm{He} + n, & (0.11 \pm 0.02)\% < w < (0.16 \pm 0.02)\%; \end{cases} \\ {}^{14}\mathrm{N}(\mu^-, \nu){}^{8}\mathrm{Li}\,{}^{6}\mathrm{Li}, \quad w < (1.4 \cdot 10^{-2})\%; \\ {}^{16}\mathrm{O}(\mu^-, \nu){}^{8}\mathrm{Li}\,{}^{7}\mathrm{Be}\,n, \quad w < (1.5 \cdot 10^{-2})\%; \\ {}^{12}\mathrm{C}(\mu^-, \nu)\,2\alpha{}^{3}\mathrm{H}n, \quad w \leqslant (2.0 \pm 0.2)\%. \end{array}\right\} \quad (1)$$

Measurement of the angular correlations of the reaction products made it possible to establish the mechanism of the process in a number of cases. Examples of such analysis are given in Figs. 2 and 3. The angular correlation between $^3$He and the neutral particles in the reaction $^{12}C(\mu^-, \nu)^8Li^3He\,n$ indicates that the $n$ and $^3$He are formed by the breakup of $^4$He* (see Fig. 2).

The use of methods that make it possible to investigate processes with the emission of charged particles from individual isotopes considerably augments the information obtained from photoemulsions. Although no systematic investigations are yet available, some information has been obtained.

The chamber method has been used to investigate the channel with the emission of charged particles in neon. In one case a liquid-hydrogen chamber with small neon admixture[12] was used; in the other, an isotropic spark chamber filled with neon at atmospheric pressure.[13] The first method detected only those events in which a fast charged particle was produced. The probability of this process was found to be (3.2±0.5)%. The second method detected charged particles in a wide energy interval, beginning at ranges equal to that of a 1.1 MeV proton. In this case, the probability was appreciably higher at (20±4)%. Comparison of these two results indicates that the charged particles emitted as a result of the capture of muons by neon have mainly low ener-

TABLE III. Relative probability (%) of formation of $n$-prong stars from muon capture by the light and heavy components of the photoemulsion (Ref. 6.)

| Number of prongs | Light component | Heavy component |
|---|---|---|
| 1 | 5.7±4.0 | 94.3±4.0 |
| 2 | 68.2±2.1 | 31.8±2.7 |
| 3 | 88.6±2.5 | 11.4±2.5 |
| 4 | 97.7±2.3 | 2.3±2.3 |
| All stars | 20.4±3.6 | 79.6±3.6 |

[2)] Neither criterian is rigorous, which may result in small uncertainties in the classification of events.

TABLE IV. Probability of emission of charged particles (%) per capture event in the heavy and light components of the photoemulsion (Ref. 6.)

| Number of prongs | Light component | Heavy component |
|---|---|---|
| 1 | 1.5±1.1 | 2.7±0.2 |
| 2 | 3.7±0.3 | 0.17±0.02 |
| 3 | 1.7±0.1 | 0.02±0.005 |
| 4 | 0.5±0.08 | ⩽0.001 |
| Totals | 7.4±1.4 | 2.9±0.2 |

gies. In neither case were the charge or mass of the particles determined.

In the case of the nucleus $^{28}$Si, the yield of charged particles[14] is also fairly high, (15 ± 2)%. In Ref. 14, the particles were not distinguished, but Sobottka and Wills assume that it is mainly protons that are emitted. Assuming this, they evaluated the spectrum of the emitted particles, which was measured by means of an Si(Li) system which served simultaneously as target and detector. The resulting spectrum is given in Fig. 4 and clearly reveals a maximum at 2.5 MeV followed by an exponential decay.

The high-energy part of the charged-particle spectrum was analyzed in Ref. 15. The system of semiconductor detectors made it possible to determine the charge and mass of the particles and measure their energy. Measurements were made for four nuclei: Si, S, Ca, and Cu. The method made it possible to detect only the high-energy part of the spectrum: protons with $E > 15$ MeV, deuterons with $E > 18$ MeV, and tritium nuclei with $E > 24$ MeV. Measurements were made for several values of the threshold energy. The results are summarized in Table VII and displayed in Fig. 5.

This part of the spectrum is characterized by the following features:

1) the larger the mass of the charged particle, the smaller its emission probability; effectively, the spectrum contains only protons and deuterons;

2) with increasing charge $Z$ of the target nucleus, the fraction of deuterons in the total yield of charged particles decreases;

3) the proton yield has a maximum in the region of calcium, $Z = 20$;

4) the energy spectra of the charged particles extends to 50–60 MeV and is characterized by a smooth exponential dependence. To within the limits of the measurement errors, the spectra of protons from S and Ca nuclei agree with the neutron spectra measured in Ref. 16, but deviate rather strongly from the spectra given in Ref. 17.

TABLE V. Total yield (%) of charged particles from muon capture by nuclei of the light and heavy components of the photoemulsion.

| Light component | Heavy component | Literature |
|---|---|---|
| 12.9 | 2.7 | [3] |
| 15.0±2.3 | 3.1±0.4 | [5] |
| 7.4±1.4 | 2.9±0.2 | [6] |

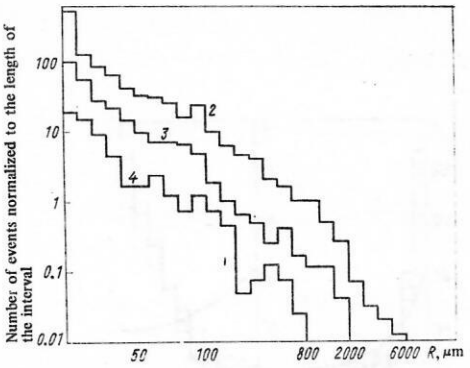


FIG. 1. Distribution of charged particles with respect to the range $R$ in muon capture by photoemulsion nuclei (2, 3, and 4 are the number of prongs in the star).

The radiochemical method made it possible to determine the probability of emission of one proton with the formation of the daughter nucleus in subthreshold states in the reactions

$$\left.\begin{aligned}\mu^- + {}^{28}\mathrm{Si} &\to p + \nu_\mu + {}^{27}\mathrm{Mg};\\ \mu^- + {}^{39}\mathrm{K} &\to p + \nu_\mu + {}^{38}\mathrm{Cl}.\end{aligned}\right\} \quad (2)$$

The problem is facilitated by the fact that both nuclei $^{27}$Mg and $^{38}$Cl are long lived. The relative probability of the channels (2) was found to be fairly high[18]:

$$w_p\,(^{28}\mathrm{Si}) = (5.3 \pm 1.0)\%; \quad (3)$$

$$w_p\,(^{39}\mathrm{K}) = (3.2 \pm 0.6)\%. \quad (3a)$$

Comparing the results of the two experiments of Refs. 14 and 18, we can conclude the following: While the main channel with the emission of charged particles accompanying muon capture by $^{28}$Si is the proton channel, the greater part of the protons are accompanied by the emission of neutrons. This channel was established by the radiochemical method in the process[19]

$$^{27}\mathrm{Al}\,(\mu^-, \nu p2n)\,^{24}\mathrm{Na},$$

with probability (3.5 ± 0.8)%. The emission of more complicated formations ($\alpha$ particles) was established in the case of capture by Ni nuclei [the target consisted of the natural mixture of $^{58}$Ni (67.8%) and $^{60}$Ni (26.2%) isotopes]; at total intensity 5% (Table VIII) the main channel was found to be $^{58}$Mi($\mu^-$, $\nu\alpha$)$^{54}$Mn (1.9 ± 0.2)%.

TABLE VI. Relative yield (%) of singly charged particles in muon capture by photoemulsion nuclei (Ref. 5).

| Particle species | C, N and O | Ag and Br | Total yield |
|---|---|---|---|
| Protons | 0.44±0.15 | 0.86±0.06 | 0.79±0.06 |
| Deuterons | 0.56±0.15 | 0.14±0.06 | 0.21±0.06 |

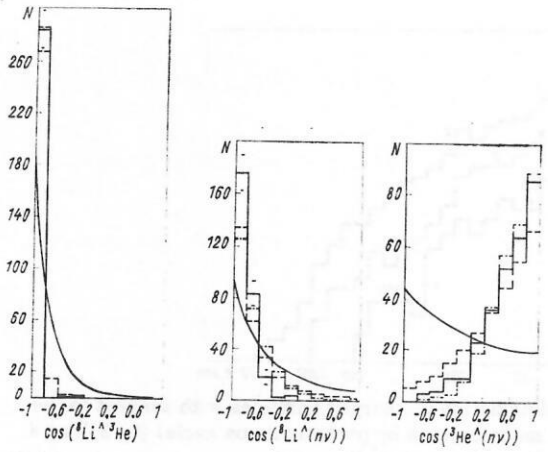

FIG. 2. Angular correlations in the process $^{12}C(\mu^-, \nu)^8Li^3He\,n$. The solid histogram gives the results of the measurements; the continuous curve shows the phase volume; the dashed histograms are the results of calculation in accordance with the scheme $\mu^-{}^{12}C \to {}^{22}B^*\nu$ with the subsequent decay chain $^{12}B^* \to {}^8Li + {}^4He^*$, $^4He^* \to {}^3He + n$; the dot-dash-dot histograms are the results of calculation under the assumption of a cluster nature ($^4$Li) of muon capture.

Detection of $\gamma$ rays resulting from the decay of excited states of the daughter nuclei with subsequent analysis of the emission spectra ($\gamma$ spectrometry) also permits one to establish with considerable confidence the final reaction products accompanying muon capture and to determine the relative intensity of the various channels. Note that in principle this method does not permit one to obtain data about the population of the ground states of the daughter nuclei, but in many cases this does not result in a loss of information because the spin of the ground state of the daughter nucleus is fairly large, and it is therefore populated with low probability.

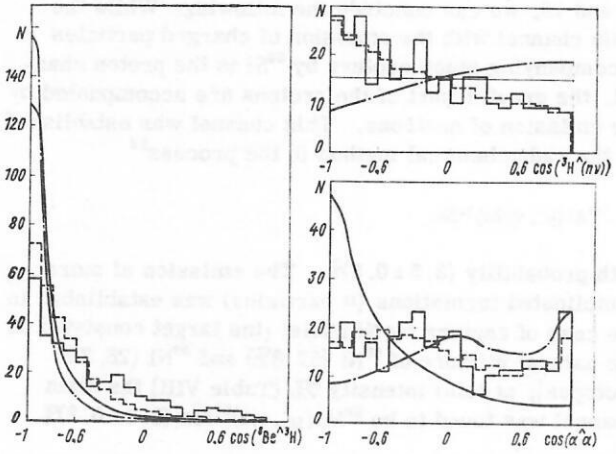

FIG. 3. Angular correlations in the process $^{12}C(\mu^-, \nu)^4He^4He^3H\,n$. The solid histogram gives the results of the measurements; the continuous curve, the phase volume; the dashed histograms, the calculation in accordance with the scheme $\mu^-{}^{12}C \to {}^{12}B^*\nu$ with the subsequent decay chain $^{12}B^* \to {}^{11}B^* + n$. $^{11}B^* \to {}^8Be^* + {}^3H$, $^8Be^* \to {}^4He + {}^4He$; the dot-dash-dot histogram, the result of calculation in accordance with the same scheme, but with the chain $^{12}B^* \to {}^8Be^* + {}^4H^*$, $^4H^* \to {}^3H + n$, $^8Be^* \to {}^4He + {}^4He$.

As an example, Fig. 6 shows the level scheme of the daughter nuclei formed as a result of muon capture by $^{40}$Ca. The main muon-capture reaction channel is, naturally, associated with the formation of the $^{39}$K nucleus in various states. But at the same time the experiments of Refs. 21 and 22 revealed lines corresponding to $\gamma$ transitions in the nuclei $^{39}$Ar, $^{38}$Ar, and $^{38}$Cl, which can be formed only if a charged particle is emitted in the muon-capture process. The probabilities of excitation of the states of these nuclei found by analyzing the $\gamma$ spectra are given in Table IX.

The large number of $\gamma$ transitions and their cascade nature lead frequently to superposition of lines, which makes it much harder to decipher the spectra. This is one of the main factors responsible for the discrepancy between the results of analysis of measurements with one and the same nucleus made by different experimental groups (which is already reflected in the data in Table IX). The results of measurements of the yield of $\gamma$ rays from Ar and Cl nuclei reveal an appreciable contribution of the channel with the emission of charged particles in the process of disintegration of the $^{40}$Ca nucleus by muons.

Analogous results were also obtained in the investigation of muon capture by $^{24}$Mg, $^{28}$Si, $^{56}$Fe, and $^{58}$Ni (see Tables VIII and X). These measurements confirm the results obtained by the direct method. It is characteristic that the probability of emission of only one proton is equal to or even less than the probability of emission of a proton accompanied by one or several neutrons.

For a number of odd nuclei in the region of mass numbers $A = 45-93$ ($^{45}$Sc, $^{55}$Mn, $^{59}$Co, and $^{93}$Nb) $\gamma$ spectrometry[24] gives an intensity of the channel with charged-particle emission not exceeding 1%. In the case of heavier nuclei, charged particles were either not observed ($^{151}$Eu, $^{153}$Eu) (Ref. 25) or their yield did not exceed 1–2% ($^{127}$I, $^{209}$Bi, $^{142}$Ce, $^{140}$Ce, $^{138}$Ba, and $^{120}$Sn) (Refs. 24 and 26).

## 2. SOME GENERAL FEATURES OF MUON CAPTURE ACCOMPANIED BY THE EMISSION OF CHARGED PARTICLES

From the complete set of experimental data, we can deduce some general features of the process of muon

TABLE VII. Probabilities of emission of fast protons, deuterons, and tritons (%) per capture event in the nuclei $^{28}_{14}$Si, $^{32}_{16}$S, $^{40}_{20}$Ca, and $^{64}_{29}$Cu.

| Threshold energy, MeV | $^{28}_{14}$Si | | | $^{32}_{16}$S | | |
|---|---|---|---|---|---|---|
| | $p$ | $d$ | $t$ | $p$ | $d$ | $t$ |
| 15 | 0.88±0.06 | — | — | 1.15±0.09 | — | — |
| 18 | 0.64±0.05 | 0.33±0.03 | — | 0.78±0.07 | 0.34±0.04 | — |
| 24 | 0.33±0.03 | 0.15±0.02 | 0.02±0.01 | 0.42±0.05 | 0.17±0.03 | 0.04±0.01 |
| 42 | 0.04±0.01 | 0.02±0.01 | — | 0.06±0.01 | 0.01±0.01 | — |
| | $^{40}_{20}$Ca | | | $^{64}_{29}$Cu | | |
| | $p$ | $d$ | $t$ | $p$ | $d$ | $t$ |
| 15 | 1.30±0.11 | — | — | 0.60±0.07 | — | — |
| 18 | 0.94±0.08 | 0.26±0.04 | — | 0.46±0.06 | 0.10±0.03 | — |
| 24 | 0.48±0.06 | 0.19±0.03 | 0.02±0.01 | 0.27±0.05 | 0.08±0.03 | 0.005±0.005 |
| 42 | 0.06±0.02 | 0.02±0.01 | — | 0.04±0.02 | 0.02±0.01 | — |

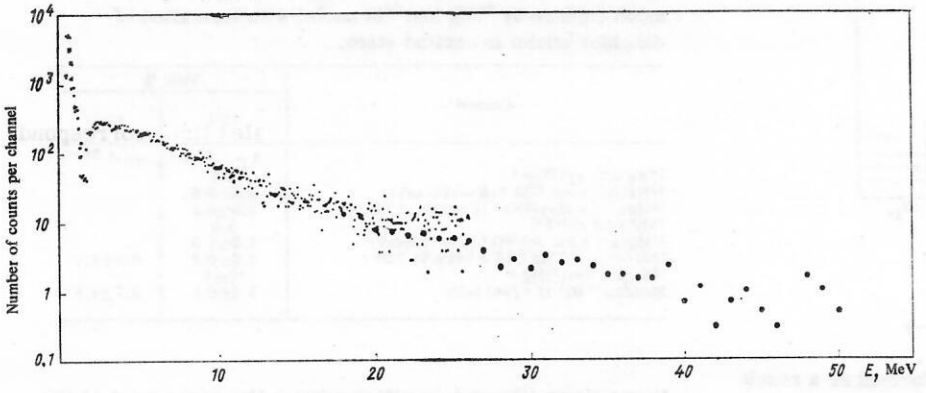


FIG. 4. Energy spectrum of charged particles (mainly protons) in muon capture by the nucleus $^{28}$Si in the region $E < 20$ MeV (Ref. 14) and in the region $E > 20$ MeV (Ref. 15).

capture accompanied by the emission of charged particles. The integral yield of charged particles from nuclei of the $1p$ shell ($^{12}$C–$^{16}$O) is about 10%. In nuclei of the $2s$–$1d$ shell ($^{20}$Ne–$^{40}$Ca), the contribution of this channel is larger, reaching 15–20%. The yield of charged particles remains at about the same level in the case of the somewhat heavier even–even nucleus $^{58}$Ni. However, for the odd nuclei in this range of mass numbers $A$ these values already decrease considerably. For the nuclei Br and Ag in the photoemulsions the yield of charged particles is 2.9%, while in nuclei with mass number $A > 100$ it does not exceed 1–2%. The maximal yield occurs in the region of $^{20}$Ca.

The charged-particle spectrum is basically soft. The conclusion to be drawn from this is that the charged-particle emission is associated with secondary processes that take place in the excited intermediate nucleus.

The Coulomb barrier for nuclei with mass number $A = 60$ reaches a height of 8 MeV, which strongly hinders the emission of slow secondary particles if they are charged. It is therefore not surprising that the yield of charged particles accompanying muon capture in heavy nuclei is small.

The contribution of the hard component to the total spectrum of charged particles is small and does not exceed 2–3%. The yield of high-energy particles also peaks in the region of nuclei with $Z = 20$.

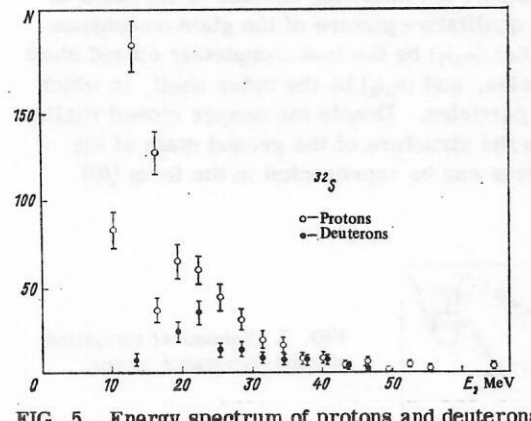


FIG. 5. Energy spectrum of protons and deuterons in muon capture by the $^{32}$Si nucleus.[15]

The high-energy component may be due either to the cluster capture mechanism (quasideuteron, biproton, $\alpha$-particle, etc) or to the effect of rescattering of fast neutrons formed by the direct capture process.

In light and medium nuclei, charged-particle emission is accompanied rather often by the emission of one or several neutrons. The emission of two or several nucleons is characteristic of the cluster capture mechanism, in which at least one of the emitted particles must be fast. Secondary processes in the intermediate nucleus can also lead to the emission of several particles, but in this case they are more likely to be soft. Therefore, to establish the mechanism of the process, it is necessary to investigate the energy and angular distributions of the emitted particles.

## 3. THEORETICAL ANALYSIS OF MUON CAPTURE ACCOMPANIED BY THE EMISSION OF CHARGED PARTICLES

The capture of muons by nuclei takes place predominantly through the excitation of collective states of the type of giant resonances. The decay of giant-resonance states leads to the formation of the main part of the neutron spectrum. The theory created to describe the phenomenon of resonance capture of muons encompasses a large number of questions associated with the decay of collective states accompanied by the emission of neutrons: profile of the spectrum, absolute yield, population of the states of the daughter nucleus. Therefore, it is natural that the yield of charged particles can also be related to the decay mechanism of the giant-resonance states.[27]

TABLE VIII. Probability of emission of charged particles in muon capture by nickel nuclei (natural mixture) with formation of daughter nuclei in excited state.

| Channel | Yield, % | Method |
|---|---|---|
| $^{58}$Ni ($\mu^-$, $\nu pn$) $^{56}$Fe ($2^+$, $E = 847$ keV) | 9.3±1.1 | $\gamma$ spectrometry[20] |
| $^{58}$Ni ($\nu^-$, $\nu\alpha$) $^{54}$Mn *<br>$^{58}$Ni ($\mu^-$, $\nu\alpha\,2n$) $^{52}$Mn *<br>$^{60}$Ni ($\mu^-$, $\nu p$) $^{59}$Fe *<br>Other channels | 1.9±0.2<br>0.56±0.06<br>0.12±0.01<br>1.5 | Radiochemical[19] |
| $^{56}$Fe ($\mu^-$, $\nu\,pn$) $^{54}$Cr ($2^+$, $E = 835$ keV) | 2.9±0.6 | $\gamma$ spectrometry[20] |

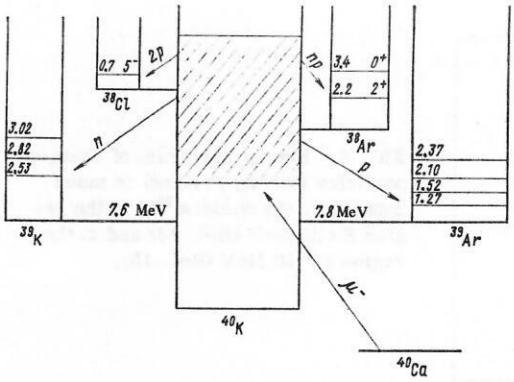


FIG. 6. Level scheme of daughter nuclei formed as a result of muon capture by the $^{40}$Ca nucleus.

A giant resonance is formed from several groups of transitions. This is shown schematically in Fig. 7. One group is associated with the excitation of nucleons from the outer shell and forms the main excitation branch (except for a few cases when the outer shell has only begun to fill). Another group of transitions is due to the excitation of nucleons in strongly bound shells. These transitions form the high-energy branch of the capture spectrum. The energy gap between the two branches is due to the large difference in the transition energies from the inner and the outer shells. This property of the giant resonance in photonuclear reactions was noted long ago and called configuration splitting[28] (see also Ref. 29).

Configuration splitting must also be manifested in muon capture, but we here encounter a feature associated with the nature of the energy dependence of the probability of excitation of states of the intermediate nucleus $(A, Z-1)$: In photonuclear reactions, the cross section of dipole photoabsorption is proportional to the energy of the $\gamma$ ray, i.e., to the excitation energy $E^*$ of the level, whereas as in the muon-capture reaction the probabilities of level excitation due to first-forbidden

TABLE IX. Probability of formation of excited states of the nuclei $^{39}$K, $^{39}$Ar, $^{38}$Ar, and $^{38}$Cl in muon capture by the $^{40}$Ca nucleus.

| Daughter nucleus | $E^*$, MeV | $J^\pi$ | Probability of formation, % [22] | [21] |
|---|---|---|---|---|
| $^{39}$Ar * | 1.27 | 3/2⁻ | 1.0±0.3 | 2.2±0.9 |
| | 1.52 | 3/2⁺ | 2.6±0.6 | 0.4±0.3 |
| | 2.10 | — | 0.7±0.2 | — |
| | 2.37 | 1/2⁺ | 0.5±0.2 | — |
| | 2.43 | | 0.76±0.13 | — |
| | 3.26 | | 0.32±0.19 | — |
| Total yield | — | — | 5.9 | 2.3 |
| $^{38}$Ar * | 2.17 | 2⁻ | 3.1±0.4 | 6±3 |
| | 3.38 | 0⁺ | 0.94±0.16 | — |
| | 3.81 | 3⁻ | 1.52±0.15 | — |
| | 3.94 | 2⁺ | $1.2^{+0.3}_{-0.7}$ | — |
| Total yield | — | — | 6.8 | — |
| $^{38}$Cl * | 1.31 | 4⁻ | 1.05±0.17 | — |
| Total yield in excited states of the nucleus $^{39}$K | — | — | 13 | 20 |

TABLE X. Probability of emission of charged particles in muon capture by $^{24}$Mg and $^{28}$Si nuclei with formation of daughter nuclei in excited state.

| Channel | Yield, % [23] | [21] |
|---|---|---|
| $^{24}$Mg ($\mu^-$, $\nu p$) $^{23}$Ne * | 0.7 | |
| $^{24}$Mg ($\mu^-$, $\nu np$) $^{22}$Ne * ($E$ = 1247 keV) | 4.4±0.6 | |
| $^{24}$Mg ($\mu^-$, $\nu p2n$) $^{21}$Ne * ($E$ = 350 keV, 5/2⁺) | 2.5±0.3 | |
| Total yield of $^{19}$F*! | 3.4 | |
| $^{24}$Mg ($\mu^-$, $\nu 3p$, $3n$) $^{18}$O * ($E$ = 1979 keV) | 1.9±1.0 | |
| $^{28}$Si ($\mu^-$, $\nu p$) $^{27}$Mg * ($E$ = 984 keV) 3/2⁺ | 1.9±0.2 | 0.4±1.0 |
| $^{28}$Si ($\mu^-$, $\nu pn$) $^{26}$Mg * | 10±1 | |
| Including $^{26}$Mg* ($E$ = 2940 keV) | 3.2±0.5 | 2.7±1.8 |

transitions (these transitions form the main part of the capture spectrum in light and medium nuclei) are effectively proportional to $E_\nu^4 = \{m_\mu - (E^* - E_0)\}^4$, which decreases rapidly with increasing $E^*$. This means that unless the excitation of the high-energy branch in muon capture is enhanced by the axial current it will be fairly weak. In the nuclei in the middle and at the end of the $1p$ shell there is no such enhancement, and a small fraction of the total capture probability corresponds to the high-energy part of the capture spectrum. Theoretical analysis of the excitation spectrum of the nuclear system resulting from capture of muons by nuclei of the $1p$ shell shows that the giant resonance in these nuclei is very broad and covers the region from 10 to 25–30 MeV and more. A typical example of the resonance in the case of muon capture by nuclei of the $1p$ shell is shown in Fig. 8 (Ref. 30) for the example of the reaction $\mu^- + {}^{14}\mathrm{N} \to {}^{14}\mathrm{C}^* + \nu$. Note that in this case about 3% of the total capture probability corresponds to the high-energy part of the spectrum ($E^* \geq 23$ MeV).

In nuclei of the $2s-1d$ shell, the high-energy excitation branch is enhanced by the transition $1p_{3/2}-1d_{3/2}$ from the deep $1p$ shell as a result of the predominantly axial-vector current.[31] Because of this particular feature of the excitation, about 15% of the intensity is due to the high-energy part of the spectrum. As an example, we give in Table XI the main transitions and the structure of the states that form the giant resonance in the reaction $\mu^- + {}^{32}\mathrm{S} \to {}^{32}\mathrm{P} + \nu$. In contrast to the nuclei of the $1p$ shell, in this case the excitation spectrum clearly reveals the enhancement of the high-energy branch.

In the framework of the microscopic approach based on the shell model the following scheme is adequate to describe the qualitative picture of the giant-resonance excitation. Let $(n_1 j_1)$ be the last completely closed shell with $k_1$ particles, and $(n_2 j_2)$ be the outer shell, in which there are $k_2$ particles. Denote the deeper closed shells by (0). Then the structure of the ground state of the original nucleus can be represented in the form $\{(0)$

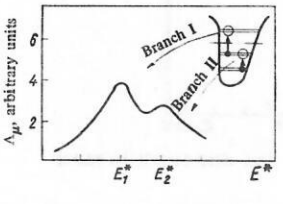


FIG. 7. Scheme of formation of giant-resonance states.

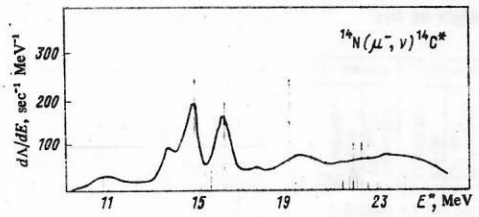


FIG. 8. Excitation spectrum of nuclear system in muon capture by the $^{14}$N nucleus.

$\times (n_1 j_1)^{k_1} (n_2 j_2)^{k_2}\}$. The low-energy branch of the giant resonance is formed mainly by transitions to the states $\{(0)\ (n_1 j_1)^{k_1} (n_2 j_2)^{k_2-1}\ (n_3 j_3)^1\}$ and lies in the energy region $E_1^* = 10$–$20$ MeV. In nuclei of the $1p$ shell, this branch is formed by the transitions $1p \to 2s$ or $1p \to 1d$; in nuclei of the $2s$–$1d$ shell, by the transitions $1d_{5/2} \to (1f, 2p)$.[3] The high-energy branch of the giant resonance is formed by transitions to the states $\{(0)\ (n_1 j_1)^{k_1-1}\ (n_2 j_2)^{k_2+1}\}$ and lies in the range of energies $E_2^* > 20$ MeV. In $1p$ nuclei, these are $1s \to 1p$ transitions; in $2s$–$1d$ nuclei, $1p \to 1d_{3/2}$ transitions. Since first-forbidden and allowed transitions are predominant in muon capture by light and medium nuclei, we shall consider only these transitions.

The nature of the subsequent decay of the giant-resonance states is affected by the structural features of the resonance itself and by the states of the daughter nucleus and energy factors determined by the thresholds $\varepsilon$ for the emission of definite particle species.

The thresholds $\varepsilon$ for the emission of different particles from the intermediate nucleus $(A,\ Z-1)$ depend on the mass number $A$ and have the following values, respectively:

| nuclei in the middle and at the end of the $1p$ shell | nuclei of $2s$–$1d$ shell |
|---|---|
| $\varepsilon_n = 4$–$7$ MeV | $\varepsilon_n = 8$ MeV |
| $\varepsilon_p = 15$–$20$ MeV | $\varepsilon_p = 8$–$10$ MeV |
| $\varepsilon_\alpha = 10$–$12$ MeV | $\varepsilon_\alpha = 6$–$10$ MeV |

The pronounced difference between the thresholds for the emission of different particle species is due to the violation of the relation between the number of protons and neutrons in the intermediate nucleus.

From the values given here and the structure of the excitation spectrum of the nuclear system it follows directly that in nuclei in the middle and at the end of the $1p$ shell the channel $(A,\ Z-1)^* \to (A-1,\ Z-2) + p$ is weak because of the high position of the proton-emission threshold. In fact, a detailed calculation in the framework of the many-particle shell model for the example of the nucleus $^{14}$N shows that the intensity of the channel $^{14}N(\mu^-,\ \nu p)^{13}B$ does not exceed 1% per muon capture event.[30] In the case of muon capture by $^{32}$S, the intensity of the channel $^{32}P \to {}^{31}Si + p$ was also found on the basis of calculations to be of the order 1–2% because of the weak fractional-parentage coupling between the

[3]Excitation of nucleons of the outer subshells $2s$ and $1d_{3/2}$ leads to the formation of the nucleus $(A,\ Z-1)$ in mainly bound states.

TABLE XI. Probability of excitation of resonances and their structure in muon capture by the $^{32}$S nucleus.

| Structure of resonance | $E^*(^{32}P)$, MeV | Probability, $10^4$ sec$^{-1}$ | Relative probability, % | Structure of resonance | $E^*(^{32}P)$, MeV | Probability, $10^4$ sec$^{-1}$ | Relative probability, % |
|---|---|---|---|---|---|---|---|
| $1d_{5/2}^{-1},\ j^{40}_1,\ 1f_{7/2} : 2^-$ | 10.9 | 13.9 | 9 | $1d_{5/2}^{-1},\ j^{40}_1,\ 1f_{5/2} : 1^-$ | 17.5 | 10.9 | 7 |
| $1d_{5/2}^{-1},\ j^{40}_1,\ 2p_{3/2} : 1^-$ | 11.0 | 3.7 | 2 | $1p_{1/2}^{-1} j^5 (3/2)_1 : 1^-$ | 18.9 | 5.5 | 3.5 |
| $j^3 (5/2)_1,\ 1f_{5/2} : 1^-$ | 12.5 | 4.2 | 3 | $1p_{3/2}^{-1} j^5 (3/2)_1 : 1^-$ | 26.6 | 15.4 | 10 |
| $1d_{5/2}^{-1},\ j^{40}_1,\ 1f_{7/2} : 1^-$ | 12.6 | 10.1 | 6.5 | $1p_{3/2}^{-1} j^5 (3/2)_1 : 0^-$ | 26.7 | 3.4 | 2 |
| $1d_{5/2}^{-1},\ j^{40}_1,\ 2p_{1/2} : 2^-$ | 13.0 | 4.1 | 2.5 | $1p_{3/2}^{-1} j^5 (3/2)_2 : 0^-$ | 28.4 | 5.3 | 3.5 |
| $1d_{5/2}^{-1},\ j^{40}_1,\ 1f_{5/2} : 2^-$ | 16.4 | 4.1 | 2.5 | | | | |

giant-resonance states and the $^{31}$Si states. This behavior must also probably be exhibited in other nuclei of the $2s$–$1d$ shell.

The threshold for emission of $\alpha$ particles by the intermediate nucleus $(A,\ Z-1)$ lies much lower than the proton threshold, which in principle must favor decay through the channel $(A,\ Z-1)^* \to (A-4,\ Z-3) + \alpha$. However, as follows from the excitation scheme of the giant resonance considered earlier, we see that if the $\alpha$ particle is formed from nucleons in one shell, the final nucleus $(A-4,\ Z-3)$ is formed in a highly excited hole state, which strongly reduces the probability of decay through this channel. But if the $\alpha$ particle is formed from nucleons of different shells, the spectroscopic factors are small.

Thus, the decay of giant-resonant states in nuclei of the $1p$ and $2s$–$1d$ shells through the channels

$$(A,\ Z-1)^* \to \begin{cases} (A-1,\ Z-2) + p, \\ (A-4,\ Z-3) + \alpha \\ \text{etc.} \end{cases}$$

is a fairly rare event. Therefore, the experimentally observed large yield of charged particles must be related to some other mode of decay of the giant-resonance states.

The dominant decay channel of the low-energy branch of the resonance is the channel with emission of a neutron. In this case, excited states of the daughter nucleus $(A-1,\ Z-1)$, and not the ground state, are predominantly populated. Some of these states lie higher than the threshold for emission of the subsequent neutron or charged particle. In the nucleus $(A-1,\ Z-1)$, the thresholds of decay with the emission of different particle species are comparable, which makes possible competition between different channels. A succession of transitions of this kind was calculated[30] for muon capture by $^{14}$N, and it was found that the probability of the process

$$^{14}N\ (\mu^-,\ \nu n)\ ^{13}C^* \to p + {}^{12}B$$

is less than 1%, and that of the process

$$^{14}N\ (\mu^-,\ \nu)\ 2n3\alpha \to p + {}^{12}B$$

is about 1%.

In nuclei of the $2s$–$1d$ shell, such a calculation was

made[31] for capture by $^{32}S$. The probability of population of $^{31}P$ states above the threshold of subsequent emission of protons, i.e., the channel

$$^{32}S\,(\mu^-, \nu n)\,^{31}P \to p + {}^{30}Si,$$

for the decay of giant-resonance states due to the excitation of nucleons from the $1d_{5/2}$ subshell was found to be $\approx 2\%$.

Let us now consider the decay of the high-energy branch of the resonance. In this case, decay with emission of a nucleon $(n_2 j_2)$ and formation of the daughter nucleus $(A-1)$ also in a hole state is predominant. The center of gravity of the hole component in the $(A-1)$ nucleus lies high, and direct decay to such a level is energetically forbidden. A small admixture of this component in low-lying states of the nucleus $(A-1)$ opens this channel. However, in the nuclei in the middle and at the end of the $1p$ shell the probability of excitation of the high energy branch of the resonance is small, and therefore the yield of charged particles through this channel is very small[30]:

$$^{14}N\,(\mu^-, \nu)\,n^{13}C^* \to \text{ charged particles } w_T < 0.1\%;$$
$$^{12}C\,(\mu^-, \nu)\,n^{11}B^*$$
$$\to \begin{cases} {}^8Be + {}^3H,\ w_T \sim 1\%;\ w_E = (1.1 \pm 0.1)\%\ [11] \\ {}^8Li + {}^3H,\ w_T < 0.2\%\ \text{not observed experimentally.} \end{cases}$$

It is different for nuclei at the start at the $1p$ shell ($^6Li$ and $^7Li$). In this case, the probability of excitation of the high-energy branch of the resonance is large. Detailed calculations made for $^6Li$ show that the structural features of the states of the high-energy branch of the resonance lead to decay through the channel (see, for example, Ref. 32) $^6Li(\mu^-, \nu)^3H^3H$ with 11% probability and through the channel $^6Li(\mu^-, \nu)n^3H\,d$ with probability 20–25%.

The spectrum of tritons in the channel $^6Li(\mu^-, \nu)^3H^3H$ is shown in Fig. 9. Since the states that decay preferentially through this channel are situated slightly higher than the threshold, the spectrum of the emitted tritons is very soft. The triton spectrum calculated in the framework of the resonance approach is very similar to the spectrum calculated in the framework of the direct mechanism.[33] However, in the last case the spectrum is smooth, whereas structure is predicted on the basis of the resonance mechanism.

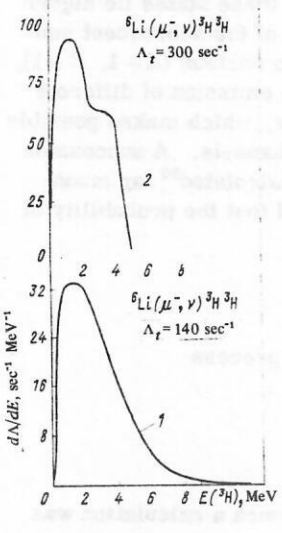


FIG. 9. Calculated spectrum of tritons in the process $^6Li(\mu^-, \nu)^3H^3H$. 1) Calculation in the framework of the direct mechanism[33]; 2) calculation in the framework of the resonance approach.[32]

TABLE XII. Probability of population of different states of the nucleus $^{31}P$.

| Levels of the nucleus $^{31}P$ | | $\alpha = 0\%$ | | $\alpha = 5\%$ | |
|---|---|---|---|---|---|
| $E^*$, MeV | $J^\pi$ | Probability, $10^3$ $sec^{-1}$ | Relative probability, % | Probability, $10^3$ $sec^{-1}$ | Relative probability, % |
| 0 | $1/2^+$ | 161 | 10.5 | 149 | 9.5 |
| 1.3 | $3/2^+$ | 53 | 3.5 | 46 | 3 |
| 2.2 | $1d_{5/2}^{-1}, j^4 0_1^+$ | 382 | 25 | 320 | 21 |
| 3.1 | $1/2^+$ | 36 | 2.5 | 33 | 2 |
| 3.3 | $5/2^+$ | 15 | 1 | 12 | 1 |
| 3.4 | $7/2^+$ | 4 | — | 2 | — |
| 3.5 | $3/2^+$ | 25 | 2 | 21 | 2 |
| 4.4 | $1d_{5/2}^{-1}, j^4 2_1^+$ | 199 | 13 | 159 | 10 |
| 6.0 | $1d_{5/2}^{-1}, j^4 0_2^+$ | 36 | 2.5 | 24 | 2 |
| 6.5 | $1d_{5/2}^{-1}, j^4 2_2^+$ | 147 | 9.5 | 110 | 7 |
| 6.7 | $1d_{5/2}^{-1}, j^4 4_1^+$ | 18 | 1 | 17 | 1 |
| 7.0 | $1d_{5/2}^{-1}, j^4 0_1^+$ | 83 | 5.5 | 33 | 2 |
| 8.1 | $1p^{-1} j^4 T = 0$ | 4 | — | 148 | 9.5 |
| 9.2 | $1d_{5/2}^{-1}, j^4 2_1^+$ | 26 | 2 | 15 | 1 |
| 10.8 | $1d_{5/2}^{-1}, j^4 0_2^+$ | 8 | — | 3 | — |
| 11.3 | $1d_{5/2}^{-1}, j^4 2_2^+$ | 9 | — | 10 | — |
| 11.5 | $1d_{5/2}^{-1}, j^4 4_1^+$ | — | — | 1 | — |
| 12.1 | $1p^{-1}, j^4 T = 1$ | 0 | — | 48 | 3 |

The high-energy branch of the giant resonance in the nuclei of the $2s-1d$ shell is due to excitation of a $1p$ nucleon and there is therefore a strong fractional-parentage coupling to states of the nucleus $(A-1,\ Z-1)$, which also have a hole in the $1p$ shell. The states of the nucleus $(A-1,\ Z-1)$ that can contain a contribution of the $1p$-hole component have negative parity and, as follows from the level scheme of the nuclei, lie in the range of energies beginning at 6–7 MeV. If one assumes[34] that the admixture of the $1p$-hole component in the low energy states of $^{31}P$ is altogether $\alpha = 5\%$, this is sufficient for the decay of the high-energy branch of the resonance in $^{32}S$ to proceed through the neutron channel completely through this component (Table XII). However, the states of the nucleus $(A-1,\ Z-1)$ containing a hole in the $1p$ shell lie above the threshold of subsequent proton emission. Thus, there arises the following decay scheme:

$$^{32}S\,(\mu^-, \nu)\,^{32}P^* \to n + {}^{31}P^*$$
$$\qquad\qquad\qquad\qquad\quad \big\lfloor\!\!\to p + {}^{30}Si$$

with probability 10–12%.

Thus, in $^{32}S$, as well as in nuclei of the $2s-1d$ shell, the emission of neutrons from the decay of the high-energy branch of the giant resonance in muon capture is accompanied by emission of a proton. This feature for nuclei of the $2s-1d$ shell has been observed experimentally, and with intensity agreeing well with the value given above.

It is different in nuclei in the middle and at the end of the $1p$ shell. Here, the total yield of charged particles

predicted by theory is several times smaller than that found experimentally. Although the latest measurements[6] have reduced this amount by almost two times, the discrepancy remains rather large. Allowance for the monopole excitation branch (allowed transitions) does not significantly alter the situation. States of the type $\{(0)\ (n_1j_1)^{k_1}(n_2j_2)^{k_2}\}$ correspond to this excitation branch. The decay of these states has been calculated in the case of $^{12}C$ with the result[35]

$$^{12}C\,(\mu^-,\ \nu)\,^{12}B^* \to \begin{cases} ^{10}B + d \sim 0.4\%; \\ ^{8}Li + \alpha \sim 0.1\%. \end{cases}$$

The discrepancy between theory and experiment in the case of the nuclei of the $1p$ shell can partly attributed to the fact that in these nuclei, as photonuclear experiments show, half of the dipole sum lies in the region of energies above 30 MeV. Because of the particular energy dependence of the muon-capture rate, this value is decreased, but certainly exceeds by several times the 3% that follows from calculations that take into account only states with energy $1h\omega$. The inclusion of more complicated components could, besides increasing the intensity with which the high-energy region is populated, lead to the appearance of new decay routes, which, ultimately, increase the yield of charged particles. However, such calculations have not yet been made. Thus, at the present time, the question of the emission mechanism of charged particles in nuclei of the $1p$ shell remains open. For its resolution, we need more detailed experimental information about the main decay channels.

The microscopic approach based on the shell model makes possible a detailed description of the structure of the giant resonance states. But this filling in of details makes the computational scheme very cumbersome, and, if calculations are to be completed, simplifications must be used. This applies particularly to calculations of the decay channels. Therefore, at a definite stage in medium and, especially, heavy nuclei, in which individual properties are weakly manifested, it is expedient to give up such a detailed description of the giant-resonance states and retain only the gross structure, which can be calculated either in the framework of simple models or by means of sum rules.

The simplest construction of the excitation spectrum of the intermediate nucleus ignores the dynamics of the process. In this case, the Hamiltonian of the muon–nuclear interaction is set equal to a constant. If, then, the single-particle neutron functions in the wave function of the resulting particle–hole system $|ph\rangle$ are chosen in the form of plane waves, the square of the matrix element of the transition from the ground state $|0\rangle$ to the excited state $|ph\rangle$ will have the form

$$|\langle ph|H_\mu|0\rangle|^2 \sim \rho(p_{pr}),$$

i.e., will be proportional to the proton momentum distribution function $\rho(p_{pr})$ in the original nucleus, and the distribution of the capture probability over the excitation spectrum of the intermediate nucleus expressed as follows:

$$d\Lambda = \rho(p_{pr})\,\delta(\varepsilon - E_\nu - E)\,\delta(\mathbf{p}_n - \mathbf{p}_\nu - \mathbf{p}_{pr})\,d^3p_{pr}d^3p_nd^3p_\nu.$$

Specifying a definite momentum distribution (Fermi distribution for $kT = 0$ or $kT > 0$, Gaussian, etc), one can readily calculate[36] the excitation spectrum of the intermediate nucleus. Assuming that the decay of the excited system takes place statistically, Ishii[36] calculated the spectrum and yield of protons and $\alpha$ particles on the basis of the capture spectrum obtained in this way. He considered the nuclei Ag and Br. In the case of $\alpha$ particles, agreement with the experiment was obtained, but the proton yield was an order magnitude too low.

To explain the experimentally observed large yield of protons, Singer[37] suggested that one should take into account the process of direct capture of muons by a correlated pair of protons in the nucleus, $\mu^- + (pp) \to p + n + \nu$, which is analogous to the well-known quasideuteron mechanism of absorption of high-energy $\gamma$ rays. The calculation shows that the yield of protons in such a process may be about 2% per capture event, which in principle explains the experimentally observed proton yield. It should, however, be borne in mind that it is difficult to estimate the reliability of these calculations since it is necessary to use rather a large number of different approximations, the majority of which are very hard to verify directly in experiments or justify theoretically.

The scheme described above for calculating the excitation spectrum of the intermediate system and the assumption of statistical decay are very crude, and one can hardly expect such a scheme to give a detailed description of the process. It can be considerably improved, either by taking into account the dynamics of the muon capture or by taking into account the possibility of emission of particles during the pre-formation stage. The estimates of Ref. 38 made in the framework of such a scheme show that allowance for the pre-equilibrium stage of the process enables one to improve the agreement between theory and experiment for the description of the spectra of the emitted particles. Systematic analysis in the framework of this scheme of the spectra and multiplicity of the emitted neutrons, and also the spectrum and yield of charged particles, yields important information about the excitation distribution in nuclei in muon-capture processes.

Calculation of direct processes in the framework of the distorted-wave method leads to two terms in the transition amplitude. One corresponds to the so-called direct diagram (Fig. 10a), which is usually taken into

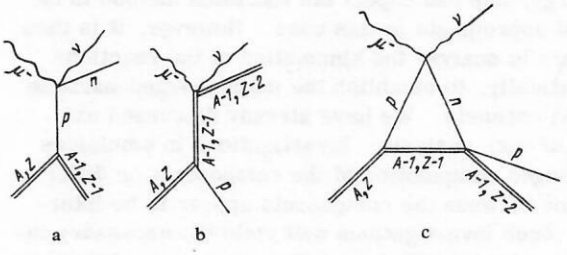


FIG. 10. Diagrams of processes of muon capture by nuclei.

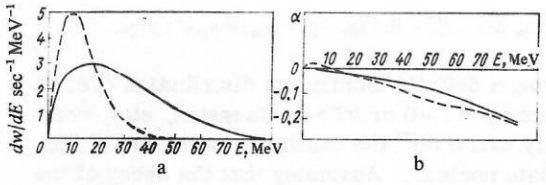


FIG. 11. Spectrum of protons and asymmetry of their angular distribution with respect to the muon spin in the process $^{16}O(\mu^-, \nu p)^{15}C(5/2^+)$. The dashed curve is the plane-wave approximation, $dW/dE \times 20$; the continuous curve takes into account interaction in the final state.

account in the distorted-wave method, while the second corresponds to the exchange diagram (Fig. 10b), which is usually ignored since it makes a small contribution. The yield of protons can be partly attributed to this last diagram (see Fig. 10c). Considering the reaction

$$\mu^- + {}^{16}O \to {}^{15}C\,(5/2^+) + p + \nu$$

on the basis of the exchange diagram, it was found in Ref. 39 that the probability of this reaction is about 0.1% when allowance is made for the interaction in the final state. If the muons in the $K$ orbit are polarized, this mechanism leads to an asymmetry of the protons with respect to the muon spin. Corresponding results are given in Fig. 11. The proton yield may also be attributed to the process of charge exchange of the neutron formed by muon capture by a proton. The diagram in Fig. 10c corresponds to this process. Observation of the $\gamma$ line from the decay of the excited $5/2^+$ state and determination of its intensity would provide information about the importance of these mechanisms of production of charged particles.

## CONCLUSIONS

We have considered a number of processes associated with the emission of charged particles in muon capture by nuclei. We can now begin to delineate the features of this process. Some of them can be understood qualitatively in the framework of the resonance mechanism of the capture process. In the first place, this applies to nuclei of the $2s-1d$ shell. The main features of the process in the case of the nuclei in the middle and at the end of the $1p$ shell cannot yet be described. These nuclei have clearly expressed individual properties, and here, in all probability, it will be necessary to analyze in detail all the main disintegration channels. In this connection, it is important to obtain additional experimental information. Bearing in mind that the charged particles emitted in muon capture mainly have low energy, one can expect the emulsion method to be the most appropriate in this case. However, it is then necessary to analyze the kinematics of the reactions systematically, to establish the main charged-particle emission channels. We have already discussed examples of such analysis. Investigations in emulsions with changed composition of the components or different ratios between the components appear to be interesting. Such investigations will yield the necessary information about the disintegration processes of the nuclei of the $1p$ shell with the emission of charged particles.

The development of schemes that take into account the pre-equilibrium stage of particle emission makes possible a detailed analysis of the disintegration processes of heavy nuclei. In this case, the approach based on a combined method may be effective, i.e., the resonance method to describe the muon capture and pre-equilibrium decay to describe the particle emission.


[1]E. P. George and J. Evans, Proc. Phys. Soc. A **64**, 193 (1951).
[2]P. Singer, Springer Tracts in Modern Physics **71**, 39 (1974); H. Uberall, Springer Tracts in Modern Physics, **71**, 1 (1974).
[3]E. F. Fry, Phys. Rev. **85**, 676 (1952); H. Morinaga and W. F. Fry, Nuovo Cimento, **10**, 308 (1953).
[4]D. Kotelchuck, Nuovo Cimento **34**, 27 (1964); D. Kotelchuck and J. V. Tyler, Phys. Rev. **165**, 1190 (1968).
[5]A. O. Vaĭsenberg *et al.*, Yad. Fiz. **1**, 652 (1965) [Sov. J. Nucl. Phys. **1**, 467 (1965)]; Yad. Fiz. **11**, 830 (1970) [Sov. J. Nucl. Phys. **11**, 464 (1970)].
[6]Yu. A. Batusov *et al.*, Yad. Fiz. **21**, 1215 (1975) [Sov. J. Nucl. Phys. **21**, 627 (1975)].
[7]A. Alumkad *et al.*, Nuovo Cimento 17, 316 (1960); R. E. E. Marshak, Meson Theory, Plenum Press, New York (1952), p. 182.
[8]Yu. A. Batusov *et al.*, Yad. Fiz. **18**, 962 (1973) [Sov. J. Nucl. Phys. **18**, 496 (1974)].
[9]G. Vanderhaeghe and M. Demeur, Nuovo Cimento Suppl. **2**, 938 (1956).
[10]Yu. A. Batusov *et al.*, Yad. Fiz. **14**, 1206 (1971) [Sov. J. Nucl. Phys. **14**, 673 (1972)].
[11]Yu. A. Batusov *et al.*, Yad. Fiz. **22**, 320 (1975) [Sov. J. Nucl. Phys. **22**, 166 (1975)].
[12]M. Schiff, Nuovo Cimento **22**, 66 (1961).
[13]V. I. Komarov and O. V. Savchenko, Yad. Fiz. **8**, 713 (1968) [Sov. J. Nucl. Phys. **8**, 415 (1969)].
[14]S. E. Sobottka and E. L. Wills, Phys. Rev. Lett. **20**, 596 (1968).
[15]Yu. G. Budyashov *et al.*, Zh. Eksp. Teor. Fiz. **60**, 19 (1971) [Sov. Phys. JETP **33**, 11 (1971)].
[16]R. M. Sundelin *et al.*, Phys. Rev. Lett. **20**, 1198 (1968).
[17]V. S. Evseev *et al.*, Yad. Fiz. **4**, 342 (1965) [Sov. J. Nucl. Phys. **4**, 245 (1967)]; M. Krieger, Preprint Columbia Univ. NEVIS-172 (1969).
[18]L. Vil'gel'mova *et al.*, Yad. Fiz. **13**, 551 (1971) [Sov. J. Nucl. Phys. **13**, 310 (1971)].
[19]G. Heusser and T. Kirsten, Nucl. Phys. A **195**, 369 (1972).
[20]H. J. Evans, Nucl. Phys. A **207**, 379 (1973).
[21]T. A. E. C. Pratt, Nuovo Cimento B **61**, 119 (1969).
[22]P. Igo-Kemenes *et al.*, Phys. Lett. B **34**, 286 (1971).
[23]G. H. Miller *et al.*, Phys. Rev. C **6**, 487 (1972).
[24]G. Backenstoss *et al.*, Nucl. Phys. A **162**, 541 (1971).
[25]C. Petitjean *et al.*, Nucl. Phys. A **178**, 193 (1971).
[26]G. R. Lucas *et al.*, Phys. Rev. C **7**, 1678 (1973).
[27]V. V. Balashov *et al.*, Proc. III Intern. Conf. on High Energy Physics and Nuclear Structure. Plenum Press, New York–London (1970), p. 174 (JINR E4-4601, Dubna (1969).
[28]V. G. Neudachin, V. G. Shevchenko, and N. P. Yudin, Phys. Lett. **10**, 180 (1964).
[29]H.-U. Jaeger, H.-R. Kissener, and R. A. Éramzhyan, in: Tudyr Seminara "Élektronnye Vzaimodeĭstviya Yader pri Malykh i Srednikh Énergiyakh" (Proc. Seminar "Electronic Interactions of Nuclei at Low and Medium Energies"), Nauka, Moscow (1973), p. 63.(Preprint JINR R4-6941, Dubna (1969)).
[30]H.-R. Kissener *et al.*, Nucl. Phys. A **215**, 424 (1973).
[31]Yu. I. Bely *et al.*, Nucl. Phys. A **204**, 357 (1973).
[32]V. A. Vartanyan and R. A. Éramzhyan, in: Voprosy Atomnoĭ

Nauki i Tekhniki (Problems of Atomic Science and Technology) (Trudy KhFTI 73-9), Khar'kov (1973), p. 25.
[33]B. R. Wienke and S. L. Meyer, Phys. Rev. C **3**, 2179 (1971); **9**, 943 (1974).
[34]R. A. Eramzhyan, R. A. Majling, and J. Řizek, Nucl. Phys. A **247**, 411 (1961).
[35]V. A. Vartanyan, M. A. Zhusupov, and R. A. Éramzhyan, Izv. Akad. Nauk SSSR **33**, 2087 (1969).
[36]C. Ishii, Progr. Theor. Phys. **21**, 663 (1959).
[37]P. Singer, Phys. Rev. **124**, 1602 (1961).
[38]T. Kozlowski and A. Zgliński, Phys. Lett. B **50**, 222 (1974); Nucleonika **19**, 72 (1974).
[39]R. A. Eramzhyan and Ya. A. Salganic, Nucl. Phys. A **207**, 609 (1973); G. E. Dogotar', Yu. A. Salganik, and R. A. Sakaev, Soobshchenie (Communication) JINR R2-9753 (1976).

Translated by Julian B. Barbour